NANO LETTERS

2007
Vol. 7, No. 3
813−817

Reversible Electrowetting on Superhydrophobic Silicon Nanowires

Nicolas Verplanck,[†] Elisabeth Galopin,[†] Jean-Christophe Camart,[†] and Vincent Thomy*,[†]

Institut d'Electronique, de Microélectronique et de Nanotechnologie (IEMN), UMR CNRS-8520, Cité Scientifique, Avenue Poincaré, BP. 60069, 59652 Villeneuve d'Ascq, France

Yannick Coffinier[‡] and Rabah Boukherroub*,[‡]

Institut de Recherche Interdisciplinaire (IRI), FRE-2963 c/o IEMN, UMR CNRS-8520, Cité Scientifique, Avenue Poincaré, BP. 60069, 59652 Villeneuve d'Ascq, France

Received November 7, 2006; Revised Manuscript Received February 2, 2007

ABSTRACT

This paper reports for the first time on the reversible electrowetting of liquid droplets in air and oil environments on superhydrophobic silicon nanowires (SiNWs). The silicon nanowires were grown on Si/SiO_2 substrates using the vapor–liquid–solid (VLS) mechanism, electrically insulated using 300 nm SiO_2, and hydrophobized by coating with a fluoropolymer C_4F_8. The resulting surfaces displayed liquid contact angle (θ) around 160° for a saline solution (100 mM KCl) in air with almost no hysteresis. Electrowetting induced a maximum reversible decrease of the contact angle of 23° at 150 V_{TRMS} in air.

Liquid actuation and manipulation on solid substrates using electrowetting is a rapidly growing field of research and has generated considerable interest from both fundamental and applied view points.[1] Electrowetting has found applications in various fields ranging from "lab-on-chip" devices[2−4] to adjustable lenses,[5] display technology,[6] fiber optics,[7] and microelectromechanical systems (MEMS).[8,9] Electrowetting-on-dielectric relies on contact angle reduction and liquid droplet motion upon application of an electric field. In a common electrowetting set up, the insulating layer is composed of an inorganic material such as SiO_2 or Si_3N_4 or organic polymers, and the hydrophobicity is induced through coating with a hydrophobic layer such as fluoropolymers or resists.[1] The main criteria required to ensure effective reversible electrowetting are that the hydrophobic layer hysteresis is as low as possible and the contact angle at zero voltage is as high as possible while the insulating layer is very thin.

The hydrophobic layers commonly used (Teflon-like and hydrophobic polymers) display contact angles below 120°. A strategy to reach higher contact angles commonly referred as "superhydrophobicity" is obtained through the combination of surface roughness with water repellent chemical coatings. The superhydrophobicity depends on both the geometrical micro- or nanostructures and the chemical composition of the surface. The surface roughness increases the amount of air trapped within the pores, while the chemical coating lowers the free surface energy (Cassie Baxter model). This effect is well-known in natural systems as the "lotus effect".[10,11] The lotus leaves' capability to remain clean from dirt and particles is attributed to the superhydrophobic nature of the leaves' surface. The surface is composed of micro- and nanostructures covered with a hydrophobic wax, responsible for the contact angle higher than 150° observed in these natural leaves. However, artificial superhydrophobic surfaces can also be achieved by several means, including generating of rough surfaces coated with low surface energy molecules,[12−20] roughening the surface of hydrophobic materials,[21−23] and creating well-ordered structures using micromachining and etching methods.[24−26]

Up to now, there are only few reports in the literature on the electrowetting on superhydrophobic nanostructured surfaces.[16,27,28] A method for dynamic electrical control over the wetting behavior of liquid droplets on superhydrophobic nanostructured surfaces prepared by etching microscopic array of cylindrical nanoposts into the surface of a silicon wafer was first demonstrated by Krupenkin et al.[27] They found that the wetting properties of the surface can be tuned from superhydrophobic behavior to nearly complete wetting as a function of applied voltage and liquid surface tension,

* Corresponding authors. E-mail: vincent.thomy@iemn.univ-lille1.fr (V.T.); rabah.boukherroub@iemn.univ-lille1.fr (R.B.). Telephone: +33 (0)3 20 19 79 51. Fax: +33 (0) 20 19 78 98.
[†] Institut d'Electronique, de Microélectronique et de Nanotechnologie.
[‡] Institut de Recherche Interdisciplinaire.

10.1021/nl062606c CCC: $37.00
Published on Web 02/16/2007

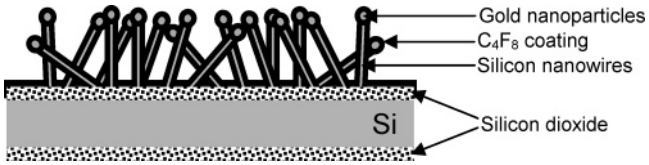

Figure 1. Schematic illustration of the microsystem used in this work. It shows silicon nanowires grown on Si/SiO_2 substrates, electrically insulated with 300 nm silicon dioxide and hydrophobized with C_4F_8. The silicon nanowires are terminated with gold nanoparticle according to the VLS mechanism growth and coated with the fluoropolymer layer.

but with no reversible effect. Electrowetting on patterned layers of SU-8 photoresist with an amorphous Teflon-AF coating was examined by Newton et al.[16] After a cycle from 0 to 130 V and back to 0 V, a decrease of the contact angle from its original value ($\theta = 152°$) to 114° was observed. The contact angle continued to fall down even when the voltage was reduced, which is a good indication of the nonreversibility of the system. Finally, the electrowetting of vertically aligned superhydrophobic carbon nanofibers was investigated by Heikenfeld et al.[28] The nanostructured material exhibited a water contact angle of 160° in air for saline solution with an *irreversible* behavior, while a *reversible* wetting was observed for a two-liquid saline/dodecane system. From these experimental data, it is clear that generating wetting reversibility in air on superhydrophobic surfaces is not only a technical challenge, but a real asset for potential applications of the structures in various fields including microfluidics, optical, and lab-on-chip devices.

This paper describes a strategy to achieve effective reversible electrowetting of liquid droplets (deionized water and two saline solutions) in oil (undecane bath) and in air on superhydrophobic silicon nanowires. Superhydrophobicity was obtained by the combination of the high roughness of SiNWs grown on silicon dioxide layer with physical coating using a fluoropolymer C_4F_8. A water contact angle of 160° was observed at zero voltage in air. The contact angle decreased to 137° when a voltage of 150 V_{TRMS} was applied and returns back to its initial value when the voltage is turned off. The reversible behavior of the system was tested by repeating the cycle (0 up to 150 V_{TRMS}) a thousand times without any apparent decrease of the contact angle.

All cleaning and etching reagents were clean-room grade. All chemicals were reagent grade or higher and were used as received unless otherwise specified.

Single-side polished silicon (100) oriented n-type wafers (Siltronix, France) (phosphorus-doped, 5−10 Ohm·cm^{-1} resistivity) were used as substrate. A dielectric layer (SiO_2) of 300 nm thickness was grown on each side of the silicon substrate by thermal oxidation (Figure 1). The resulting substrate was then degreased in acetone and isopropyl alcohol, rinsed with Milli-Q water, and cleaned in a piranha solution (3:1 concentrated H_2SO_4/30% H_2O_2) for 15 min at 80 °C followed by copious rinsing with Milli-Q water. The surface was further dried under a stream of nitrogen.

(Caution: piranha solution reacts violently with organic materials; it must be handled with extreme care, followed by copious rinsing with deionized water.)

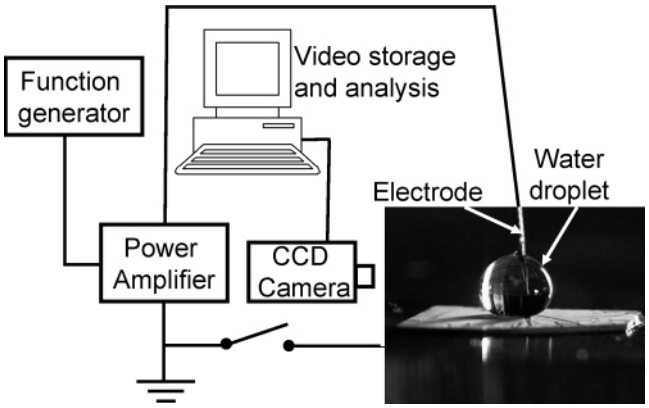

Figure 2. Experimental set up of electrowetting characterization in air.

Silicon nanowires (SiNWs) used in this work were prepared using the vapor−liquid−solid (VLS) mechanism.[29] The fundamental process is based on metal-catalyst-directed chemical vapor deposition of silicon. First, a thin film of gold (4 nm thick) was evaporated on the clean Si/SiO_2 substrate. Gold nanoparticles with a wide size distribution were obtained as a result of metal dewetting on the surface. Exposure of the gold-coated surface to silane gas at a pressure of 0.4 T ($Q = 40$ sccm) at 500 °C for 60 min led to SiNWs growth. Figure 1 shows the set up used for the EWOD experiment. The silicon nanowires were grown on Si/SiO_2 substrate electrically insulated with 300 silicon dioxide layer. The nanowires are terminated by gold nanoparticles according to the VLS mechanism. The superhydrophobicity was achieved through coating of the nanowires with C_4F_8. Both the nanowires and the gold nanoparticles terminating the nanowires are covered with the fluoropolymer.

The morphology of the nanowires was investigated by using scanning electron microscopy (SEM). Electron microscopy was carried out with a LEO 982 field-emission scanning electron microscope (SEM) with an image resolution of 2.1 nm at 1 kV and 1.5 nm at 15 kV at the analytical working distance.

Figure 2 illustrates the schematic representation of the experimental bench used to characterize the behavior of the liquid droplets under applied voltage. The material to be tested was placed on a movable stage and a liquid droplet (volume 5 μL in air and 12 μL in oil) was then deposited on its surface. A function generator (GF265 model, Centrad, France) producing a square ac signal ($V_{TRMS} = V_{pp}/2$) with a frequency of 1 kHz connected to a power amplifier (2340 model, Tegam, USA) is linked to a needle electrode in contact with the droplet. Applied voltages were comprised between 0 and 150 V_{TRMS}. We used a remote-computer-controlled goniometer system (Digidrop, GBX, France) to measure the contact angles. It is composed of a CCD camera and a video recorder (25 frames/s). The accuracy is ±1°. All measurements were made in ambient atmosphere at room temperature. Three different solutions have been tested: deionized water and saline solutions with two KCl concentrations (14 mM and 100 mM). Undecane was used for manipulation in an oil environment.

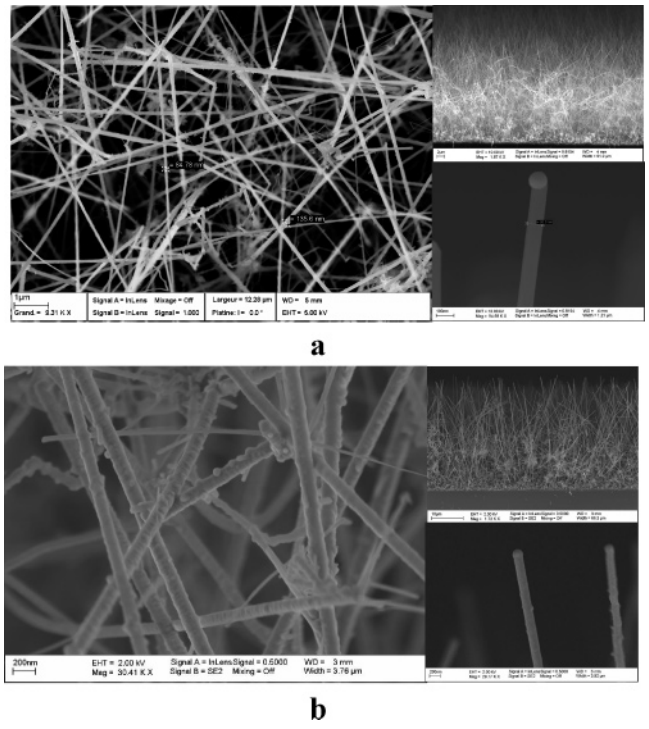

Figure 3. (a) SEM image of silicon nanowires grown on Si/SiO_2 using the vapor−liquid−solid (VLS) mechanism ($P_{SiH_4} = 0.4$ T, $T = 500$ °C, $t = 60$ min). (b) SEM image of the same silicon nanowires coated with C_4F_8.

Figure 3a displays a SEM image of the synthesized nanowires. It clearly shows a high density of SiNWs on the substrate with an average diameter in the range of 20−150 nm and 30 μm in length, leading to a nonuniform structured surface. The wide distribution of the nanowires size is related to the size of the gold nanoparticles catalyst formed during the dewetting of the Au film on the silicon dioxide layer at high temperatures. This behavior is common for Au nanoparticles prepared by a physical methodology, consisting of the thermal evaporation of a thin Au film and its successive annealing.[30] The resulting nanowires were terminated by gold nanoparticles, in agreement with the VLS growth mechanism.

Freshly prepared SiNWs were covered with a thin layer of silicon dioxide upon exposure to ambient atmosphere and thus display hydrophilic character. This means that a water droplet deposited on the surface wets completely the nanowires layer. To perform electrowetting experiments and achieve surface superhydophobicity, the SiNWs were coated with amorphous fluoropolymer like Teflon-AF (Dupont, USA) or Cytop (AGC, Japan) using the spin-coating technique. Under these conditions, we found that such fluoropolymers did not fully cover the nanowires surface. Next, the fluoropolymer C_4F_8 was deposited using a plasma technique to yield a conformal hydrophobic layer (∼60 nm thick) (Figure 3b). The resulting nanowires are totally coated with a C_4F_8 thin layer without affecting the surface roughness. It is important to note that both the nanowires and the gold nanoparticles terminating the nanowires were completely insulated by the thin fluoropolymer layer. The obtained surfaces are superhydrophobic, with a water contact angle around 160° (164° in oil) without any apparent

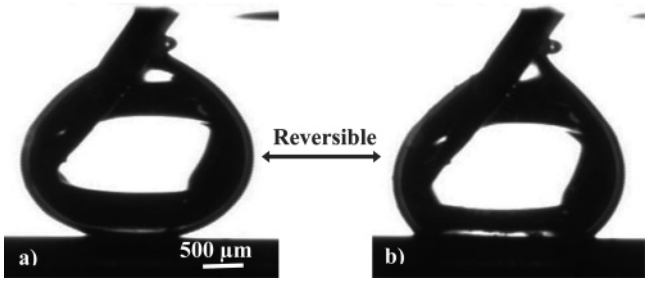

Figure 4. Electrowetting on silicon nanowires coated with hydrophobic fluoropolymer C_4F_8 displaying reversible electrowetting of a saline solution (100 mM KCl) in oil: (a) contact angle = 164° at 0 V, (b) contact angle = 106° at 150 V_{TRMS}.

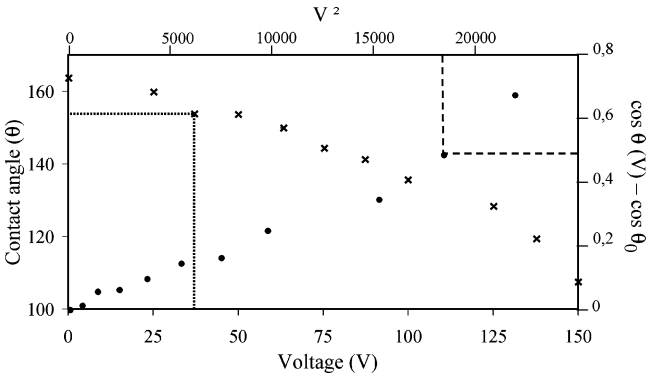

Figure 5. Contact angle vs voltage (×) and cos θ(V) − cos θ_0 vs square voltage (•) for a saline solution (100 mM KCl) in undecane. When the voltage is turned off, each point returns to its initial state.

hysteresis under our experimental conditions [precision of the measurement (±1°)]. It is to be noted that the water droplet rolls off the surface at any vibration due to the quasinull hysteresis. While superhydrophobicity is well predicted by the Cassie−Baxter relation for a structured surface, the nonuniform texturation of our surface leads to a complicated predictive calculation for the macroscopically observed contact angle.

First, the apparent contact angle of a droplet of a saline solution (100 mM KCl) in an oil bath of undecane on modified SiNWs surface was measured as a function of applied voltage. Figure 4 shows contact angles at 0 V (164°) and 150 V_{TRMS} (106°). The behavior is reversible and the contact angle returns back to its initial value at 0 V. Voltage variation from 25 to 150 V_{TRMS} led to a maximum contact angle decrease of 58° at 150 V_{TRMS} (from 164° to 106°) (Figure 5). In each case, the water droplet reacts in the same way as in Figure 4, with a repeatable wetting/relaxation cycles over 18 min (1000 cycles). No water electrolysis was found even at these high voltages, in agreement with a robust dielectric layer. A saline solution of 14 mM was next tested under the same conditions. A reversible maximum decrease of the contact angle from 164° to 127° ($\Delta\theta = 37°$) at 150 V_{TRMS} was observed. Finally when the electrowetting experiment was performed using pure deionized water, the decrease of the contact angle was quite small (9°). A contact angle of 155° was reached at 150 V_{TRMS} and saturated at this value.

Then, the wetting experiments on the superhydrophobic surface were carried out in air environment for all the

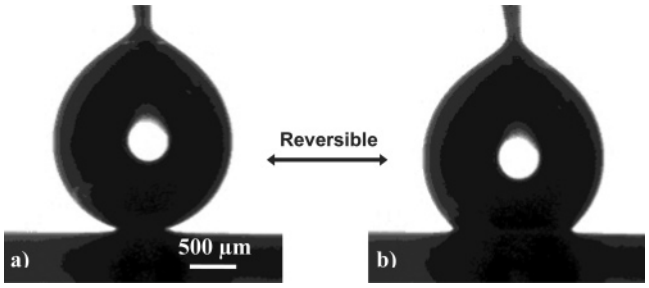

Figure 6. Electrowetting on silicon nanowires coated with hydrophobic fluoropolymer C_4F_8 displaying reversible electrowetting of a saline solution (100 mM KCl) in air : (a) contact angle = 160° at 0 V, (b) contact angle = 137° at 150 V_{TRMS}.

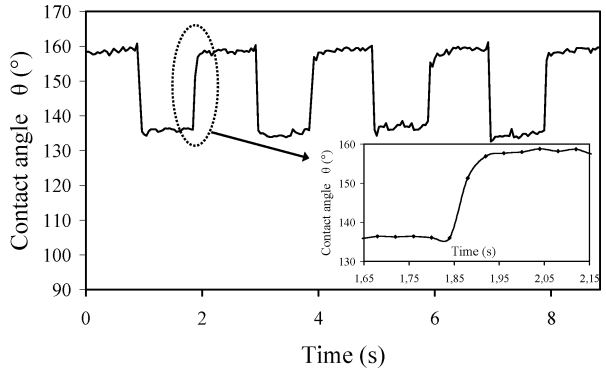

Figure 7. Contact angle vs time for a saline solution droplet (100 mM KCl) in air at 150 V_{TRMS} proving the repeatable reversibility of the electrowetting. A zoom of this curve shows the speed of the droplet relaxation: each point is a contact angle of the droplet taken from a frame of a video (25 frames/s).

solutions. As in the oil environment, reversible electrowetting was observed. After a cycle from 0 to 150 V_{TRMS}, a decrease of the contact angle from 160° to 137° was observed for a saline solution (100 mM KCl) (Figure 6). The contact angle increased back to its original value at zero voltage. Furthermore, it was demonstrated that the modified SiNWs surfaces enable reproducible wetting/relaxation cycles without any degradation of the material (highly mobile rolling ball state observed before and after experiments with the same quasinull hysteresis). Figure 7 shows part of the 1000 wetting/relaxation cycles performed over 18 min. According to the electromechanical switches speed (relay operate time of 2 ms) and to the 25 frames per s of the CCD camera, the time scale for the reversible contact angle change was estimated to be inferior to 40 ms for each cycle and is comparable to those obtained on smooth surfaces. A similar behavior of the liquid droplet on different locations of the surface was observed, indicating a uniform coating of the nanowires. Variation of the voltage from 25 to 150 V_{TRMS} under the same conditions as in Figure 5 led to a contact angle saturation at 150 V_{TRMS} (Figure 8). Saline solution of 14 mM KCl caused a decrease of the contact angle to about 139° and the latter saturated at 141° with a deionized water droplet. To the best of our knowledge, this is the first observation of reversible electrowetting on superhydrophobic surfaces in air.

Reversible electrowetting was realized on superhydrophobic silicon nanowires. The superhydrophobicity was achieved

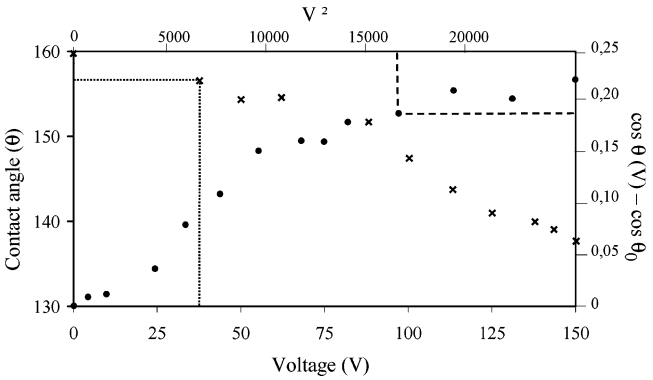

Figure 8. Contact angle vs voltage (×) and cos θ(V) − cos θ_0 vs square voltage (•) for a saline solution (100 mM KCl) in air. When the voltage is turned off, each point returns at its initial state.

using a combination of surface roughness and hydrophobization through surface coating with a fluoropolymer C_4F_8. The surface roughness combined with the low surface energy induced by the surface coating ensured air trapping between the substrate and the liquid droplets, necessary to achieve superhydrophobicity. An effective way to dynamically turn the properties of superhydrophobic nonuniform textured surface by reversible electrowetting in oil and for the first time in air, without any additional energy to the system, was demonstrated. The decrease of the contact angle upon applied voltage is equal to 58° in oil and to 23° in air for a saline solution of 100 mM KCl. It is expected that such surfaces will allow not only liquid displacement according to the quasinull hysteresis, but also droplet splitting, one of the most elementary operations in lab-on-chip devices. The obtained results will open new opportunities for designing electrowetting systems at very low voltages, with potential applications in the field of lab-on-chip and particularly in the preparation of highly functional microfluidic devices.

Furthermore, the CVD technique used for silicon nanowires growth is compatible with silicon technology and can be easily achieved on large areas. Because the growth temperature is relatively low (400−500 °C), the method can be implemented on various substrates.

Acknowledgment. We particularly thank Professors Christian Druon and Pierre Tabourier for their assistance and support. We also thank for their technical support Mrs. Patricia Lefebvre (nanowires growth) and Mr. Christophe Boyaval (SEM imaging). The European Union, the Centre National de la Recherche Scientifique (CNRS) and the Nord-Pas de Calais region are gratefully acknowledged for financial support.

References

(1) Mugele, F.; Baret, J.-C. *J. Phys.: Condens. Matter* **2005**, *17*, R705−R774.
(2) Srinivasan, V.; Pamula, V. K.; Fair, R. B. *Lab Chip* **2004**, *4*, 310.
(3) Cho, S. K.; Moon, H. J.; Kim, C. J. *J. Microelectromech. Syst.* **2003**, *12*, 70.
(4) Fouillet, Y.; Achard, J. L. *C. R. Phys.* **2004**, *5*, 577.
(5) Berge, B.; Peseux, J. *Eur. Phys. J. E* **2000**, *3*, 159.
(6) Hayes, R. A.; Feenstra, B. J. *Nature* **2003**, *425*, 383.
(7) Acharya, B. R.; Krupenkin, T.; Ramachandran, S.; Wang, Z.; Huang, C. C.; Rogers, J. A. *Appl. Phys. Lett.* **2003**, *83*, 4912.

(8) Lee, J.; Kim, C. J. *J. Microelectromech. Syst.* **2000**, *9*, 171.
(9) Yun, K. S.; Cho, I. J.; Bu, J. U.; Kim, C. J.; Yoon, E. *J. Microelectromech. Syst.* **2002**, *11*, 454.
(10) Neinhuis, C.; Barthlott, W. *Ann. Bot.* **1997**, *79*, 677.
(11) Barthlott, W.; Neinhuis, C. *Planta* **1997**, *202*, 1.
(12) Lau, K. K. S.; Bico, J.; Teo, K. B. K.; Chhowalla, M.; Amaratunga, G. A. J.; Milne, W. I.; McKinley, G. H.; Gleason, K. K. *Nano Lett.* **2003**, *3*, 1701−1705.
(13) Feng, L.; Li, S.; Li, Y.; Li, H.; Zhang, L.; Zhai, J.; Song, Y.; Liu, B.; Jiang, L.; Zhu, D. *Adv. Mater.* **2002**, *14*, 1857−1860.
(14) Feng, L.; Li, S.; Li, H.; Zhai, J.; Song, Y.; Jiang, L.; Zhu, D. *Angew. Chem., Int. Ed.* **2002**, *41*, 1221−1223.
(15) Feng, L.; Song, Y.; Zhai, J.; Liu, B.; Xu, J.; Jiang, L.; Zhu, D. *Angew. Chem., Int. Ed.* **2003**, *42*, 800−802.
(16) Herbertson, D. L.; Evans, C. R.; Shirtcliffe, N. J.; McHale, G.; Newton, M. I., *Sens. Actuators, A* **2006**, *130*−*131*, 189−193.
(17) Cao, M.; Song, X.; Zhai, J.; Wang, J.; Wang, Y. *J. Phys Chem. B* **2006**, *110*, 13072−13075.
(18) Hong, Y. C.; Uhm, H. S. *Appl. Phys. Lett.* **2006**, *88*, 244101.
(19) Tadanaga, K.; Katata, N.; Minami, T. *J. Am. Ceram. Soc.* **1997**, *80*, 1040−1042.
(20) Balaur, E.; Macak, J. M.; Tsuchiya, H.; Schmuki, P. *J. Mater. Chem.* **2005**, *15*, 4488−4491.
(21) Erbil, H. Y.; Demirel, A. L.; Avci, Y.; Mert, O. *Science* **2003**, *299*, 1377−1380.
(22) Chen, W.; Fadeev, A. Y.; Hsieh, M. C.; Oner, D.; Youngblood, J.; McCarthy, T. J. *Langmuir* **1999**, *15*, 3395−3399.
(23) Coulson, S. R.; Woodward, I.; Badyal, J. P. S.; Brewer, S. A.; Willis, C. *J. Phys. Chem. B* **2000**, *104*, 8836−8840.
(24) Fürstner, R.; Barthlott, W. *Langmuir* **2005**, *21*, 956−961.
(25) Shiu, J.-Y.; Kuo, C.-W.; Chen, P.; Mou, C.-Y. *Chem. Mater.* **2004**, *16*, 561−564.
(26) McCarthy, T. J.; Oner, D. *Langmuir* **2000**, *16*, 7777−7782.
(27) Krupenkin, T. N.; Taylor, J. A.; Schneider, T. M.; Yang, S. *Langmuir* **2004**, *20*, 3824−3827.
(28) Dhindsa, M. S.; Smith, N. R.; Heikenfeld, J.; Rack, P. D.; Fowlkes, J. D.; Doktycz, M. J.; Melechko, A. V.; Simpson, M. L. *Langmuir* **2006**, *22*, 9030−9034.
(29) Salhi, B.; Grandidier, B.; Boukherroub, R. *J. Electroceram.* **2006**, *16*, 15−21.
(30) Spadavecchia, J.; Prete, P.; Lovergine, N.; Tapfer, L.; Rella, R. *J. Phys Chem. B* **2005**, *109*, 17347−17349.

NL062606C